Design Optimization and Residual Strength Assessment of A Cylindrical Composite Shell Structure

GRANT/TR/IN/24

Report for Grant
NAG 1-2038

Period of Performance
May 1999 - April 2000

Masoud Rais-Rohani, Ph.D., P.E.
Department of Aerospace Engineering
Mississippi State University
Mississippi State, MS 39762

Phone: (662) 325-7294
Fax: (662) 325-7730
E-mail: masoud@ae.msstate.edu

Submitted to

Mechanics and Durability Branch
Mail Stop 190
NASA Langley Research Center
Hampton, VA 23681

Table of Contents

Abstract

A summary of research conducted during the specified period is presented. The research objectives included the investigation of an efficient technique for the design optimization and residual strength assessment of a semi-monocoque cylindrical shell structure made of composite materials. The response surface methodology is used in modeling the buckling response of individual skin panels under the combined axial compression and shear loading. These models are inserted into the MSC/NASTRAN code for design optimization of the cylindrical structure under a combined bending-torsion loading condition. The comparison between the monolithic and sandwich skin design cases indicated a 35% weight saving in using sandwich skin panels. In addition, the residual strength of the optimum design was obtained by identifying the most critical region of the structure and introducing a damage in the form of skin-stringer and skin-stringer-frame detachment. The comparison between the two skin design concepts indicated that the sandwich skin design is capable of retaining a higher residual strength than its monolithic counterpart. The results of this investigation are presented and discussed in this report.

Introduction

Semi-monocoque structures of the type used in aircraft fuselages are designed to meet strength and stiffness requirements with weight minimization as an underlying objective.

In such problems, the skin design is governed primarily by maximum strain, buckling and damage tolerance criteria. While the strain values can be directly extracted from the static finite element solution, the skin buckling instability assessment requires an additional eigenvalue analysis, which could be very costly within the framework of design optimization. Therefore, reliance on repeated finite-element based local buckling analysis needs to be shifted toward more practical and efficient techniques.

The technique we investigate in this research relies on the use of algebraic response models to capture the local buckling instability of skin panels.

The response surface methodology (RSM) has been used in statistical analysis for many decades, and has been gaining popularity in the structural and multidisciplinary optimization community in the past ten years. Some recent examples of these efforts are cited here.[1-3]

In its traditional sense, RSM is used to determine the values of regressor variables that optimize the response of interest. However, in our case, we are using the response models to simply predict the in-plane buckling loads of each skin panel as a function of its thickness. The ratios of the individual in-plane edge loads to the corresponding critical buckling loads are used in accordance with the stress interaction equation for formulation of skin buckling constraints.

The described technique is applied to design optimization of a semi-monocoque cylindrical structure under a combined bending-torsion loading condition. Both monolithic and sandwich skin design concepts, made of composite materials, are considered.

The finite element method is used for the static analysis of the global structural model with the internal load distribution treated as the primary field of interest. The buckling strength of individual panels is obtained using two separate response equations, one for axial and the other for shear buckling. The panel thickness is used as the only regressor in the monolithic case while the face sheet and core thickness values are used as the two regressors in the sandwich case.

A post-optimization residual strength calculation is used as a means of damage tolerance assessment of the optimal design configurations for the two skin concepts. The strain energy density criterion is used to identify the regions in the structure that are most susceptible to damage.

An artificial damage in the form of skin-stringer and skin-stringer-frame joint failure is then introduced. With buckling as the strength criterion, the residual strength of the structure is determined as a function of joint detachment length in stiffener direction.

The details of the structural design optimization and the residual strength assessment are described next.

Structural Design Model

Geometry and Loading Condition

The cylindrical section shown in Fig. 1 represents our semi-monocoque structural design model. It consists of sixteen 18 in. square flat panels, sixteen 11.5 in. radius circular panels (at top and bottom), eight equally-spaced hat stringers, and five equally-spaced Zee frames. The model is under a combined bending-torsion loading condition involving one twisting and two bending moments. The loaded end is restrained against radial translation while free in the tangential and z directions. Symmetric boundary conditions are imposed at the opposite end by restraining the translation in the z direction and the rotations about x, y and z-axes.

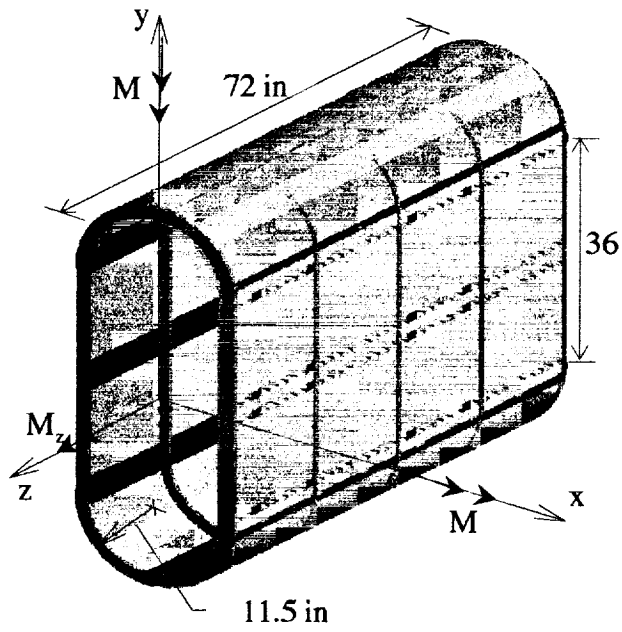

Fig. 1 Structural design geometry

Material System

For the design with monolithic skin, the entire structure is made of carbon-epoxy (IM6/SC1081) composite materials. The material properties at fiber volume fraction of 65% are as follows: X_t = 414 ksi, X_c = 270 ksi, Y_t = 7.1 ksi, Y_c = 36 ksi, S =12 ksi, E_1 = 25.7e6 psi, E_2 = 1.57e6 psi, G_{12} = 1.1e6 psi, ν_{12} = 0.27, and ρ = 0.058 lb/in^3.

In the case of the sandwich skin, the face sheets are made of IM6/SC1081 while the core is made of aluminum honeycomb. The core properties are as follows: $X_t = X_c$ = 500 ksi, $Y_t = Y_c$ = 200 ksi, S

=250 ksi, E_x = 140 ksi, E_y = 70 ksi, G_{xy} = 55 ksi, G_{xz} = 66 ksi, G_{yz} = 29.8 ksi ν_{12} = 0.3, and ρ = 0.0025 lb/in^3. The ribbon direction is assumed to be along the z-axis.

The monolithic skin laminate consists of 20 plies of equal thickness. The ply pattern we considered for the skin laminate is defined as $(45/0/-45/0/90/90/0/-45/0/45)_s$ with a blend ratio of 40%, 40% and 20% for 0°, ±45° and 90° plies, respectively. The sandwich skin design uses the same ply pattern with the core located in between the two 10-layer face sheets. The ply pattern results in a quasi-isotropic, symmetric and balanced skin laminate with no bending-twisting and shear-extension stiffness coupling.

The stringers and frames are modeled with the effective engineering properties equivalent to those of a quasi-isotropic laminate.

Finite Element Model

The finite element model of the cylindrical structure is shown in Fig. 2. The static finite element analysis is performed using MSC/NASTRAN with the pre- and post-processing done using MSC/PATRAN.

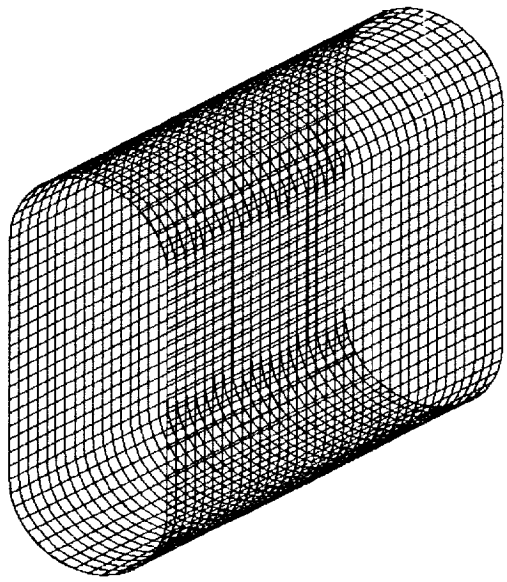

Fig. 2 Finite element model

The model shown in Fig. 2 has two types of elements, the linear CQUAD4 elements for modeling the skin and CBAR elements for modeling the stringers and frames. The structure is modeled using a total of 3,240 elements and 2,784 nodes.

The composite skin laminates are described by finite elements with PSHELL property and MAT2 material cards. The stringer and frame elements are described by PBAR property and MAT1 material cards. The stringers are assigned the smeared properties of an equivalent hat section while the frames have the smeared properties of an equivalent Zee section.

Skin Buckling Analysis

The buckling analysis described in this section only deals with the flat skin panels as shown in Fig. 3. A panel is defined here as the portion of the skin confined between two adjacent stringers and frames as indicated by the shaded area in Fig. 3. Thus, each panel is an 18-in. square section of the skin.

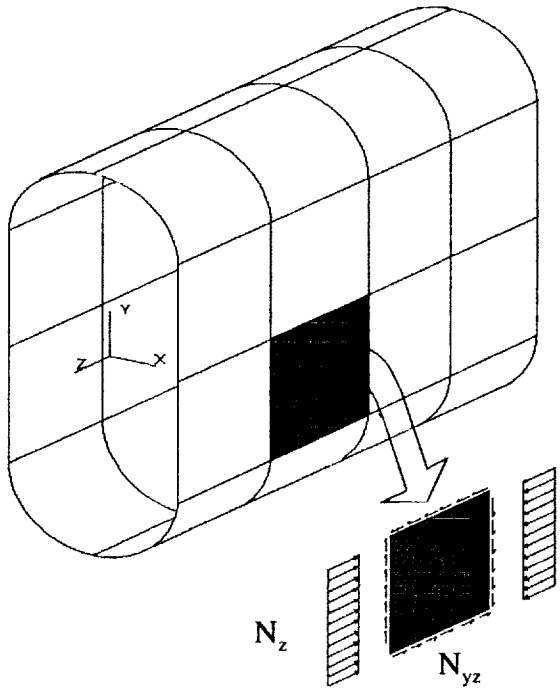

Fig. 3 Description of flat panels and associated edge loads

In the presence of a general in-plane loading, the panel buckling instability is governed by the stress interaction formula given as

$$\frac{N_y}{N_{y_{cr}}} + \frac{N_z}{N_{z_{cr}}} + \left(\frac{N_{yz}}{N_{yz_{cr}}}\right)^2 \geq 1 \qquad (1)$$

where N_y and N_z are the in-plane normal forces per unit length in y and z directions, respectively, and N_{yz} is the in-plane shear force per unit length. The terms $N_{y_{cr}}$, $N_{z_{cr}}$, and $N_{yz_{cr}}$ represent the corresponding critical buckling loads.

To examine the stability of each panel, the in-plane edge loads are obtained from the static finite element analysis of the whole structure while the corresponding critical buckling loads are obtained from the algebraic response models. The details of this procedure are described next.

In-Plane Edge Loads

The nodal forces in elements adjacent to the edges of each panel are used to determine the corresponding in-plane stress resultants N_y, N_z, and N_{yz}.

For the loading condition shown in Fig. 1, the N_y force in each panel is found to be negligible as compared to the other two. This finding is not surprising because of the absence of internal pressure. Also, the N_z force is found to vary linearly along the vertical edges of each panel as a result of M_x loading.

The variation of shear load, N_{yz} is found to be symmetric and slightly non-linear near the edges of the panel where the load is the greatest. The variation in the element shear forces from the center to the edge of each panel is found to be less than 20% for the specified loading condition.

Algebraic Response Models

Algebraic response models are used for predicting the panel buckling loads Nz_{cr} and Nyz_{cr}. Since the in-plane dimensions and the ply pattern are held fixed for each panel, the response models are formulated only in terms of panel thickness. In the case of a monolithic panel, the buckling response is captured by a quadratic polynomial in the form

$$N'_{cr} = \beta_0 + \beta_1 t + \beta_2 t^2 \tag{2}$$

To obtain the unknown coefficients in Eq. (2), a set of data for the buckling loads as a function of panel thickness is generated using the energy-based panel buckling analysis code, SCBUCKLE[4]. The panel edges are assumed to be under a uniform loading condition with simply supported boundary conditions.

We must mention at this point that the use of a code like SCBUCKLE is meant to generalize the technique described in this paper. Otherwise, for a simple design, such as a simply supported rectangular plate with a symmetric specially orthotropic lay-up ($B_{ij} = A_{16} = A_{26} = D_{16} = D_{26} = 0$), we can use the exact closed form solution available for axial and shear buckling loads[5] without the need for any approximation.

In this case, a set of 33 experiments was found to be sufficient to obtain an accurate response model for each of the two in-plane buckling loads. These experiments were conducted for a range of thickness between the lower and upper bounds of 0.1 in. and 0.5 in., respectively. The values of the coefficients found using the least squares fit technique are given in Table 1.

The quality of each response model was assessed based on the root mean square error defined as

$$\hat{\sigma} = \sqrt{\frac{SS_E}{n-p}} = \sqrt{\sum_{j=1}^{n=33} e_j^2 / 30} \tag{3}$$

where n is the total number of experiments, p is the number of coefficients in the response model, and e is the difference between the buckling load found by SCBUCKLE (treated as exact) and the approximated value found by using Eq. (2). For N_z loading case, $\hat{\sigma}$ is found to be 132.4 lb/in. compared to Nz_{cr} = 2,900 lb/in. for an average panel thickness of 0.3 in.

Table 1. Coefficients in Eq. (2)

Coeff.	Nz_{cr}	Nyz_{cr}
β_0	1,937	3,706
β_1	-24,770	-48,971
β_2	93,330	19,530

In the case of the sandwich skin panels, the face sheet thickness (t_f) as well as the core thickness (t_c) are treated as the regressor variables with the corresponding response equation expressed as

$$N'_{cr} = \beta_0 + \beta_1 t_c + \beta_2 t_f + \beta_3 t_c^2 + \beta_4 t_f^2 + \beta_5 t_c t_f \tag{4}$$

The interaction between the face sheet and core variables is captured through the coupling term in Eq. (4).

A total of 36 experiments were conducted to generate the necessary data for the shear and axial buckling loads. The core thickness was specified in the range of 0.05 in. to 0.55 in. while the thickness of each face sheet was varied from 0.003 in. to 0.033 in.

The coefficients of the polynomial in Eq. (4) are obtained using the least squares fit technique, and are listed in Table 2. The accuracy of the model was checked using various statistics including the normal probability plot of the residuals and the root mean square error.

Table 2. Coefficients in Eq. (4)

Coeff.	$N_{z_{cr}}$	$N_{yz_{cr}}$
β_0	585.8	299.4
β_1	-4,244	-5,088
β_2	-65,737	-25,806
β_3	7,065	13,204
β_4	203,412	99,901
β_5	426,711	664,100

Design Optimization Problem

The design optimization problem is formulated as:

$$\begin{aligned} &\text{Minimize:} && W(x) \\ &\text{Subject to:} && g_s(x) \geq 0, \\ & && g_b(x) \geq 0, \\ & && x^l \leq x \leq x^u \end{aligned} \tag{5}$$

where W represents the structural weight of the model in Fig. 1. The quantities g_s and g_b represent the structural strength and the buckling constraints, respectively, while x represents the vector of design variables, bounded by lower and upper limits x^l and x^u, respectively.

The optimization problem described by Eq. (5) is solved using Solution 200 of MSC/NASTRAN, which is based on the modified method of feasible directions with the sensitivity derivatives calculated using the forward finite difference scheme.

Design Variables

The structural model has a total of 8 stringers, 5 frames and 32 skin panels, of which 16 are flat and 16 are curved.

The hat stringers are assumed to have a uniform cross-section along the length of the structure with S_2, S_4, S_6 and S_8, as shown in Fig. 4, being identical to ensure cross-sectional symmetry about the x

and y axes. The condition of symmetry will make the structural design independent of the directions chosen for M_x and M_y loads.

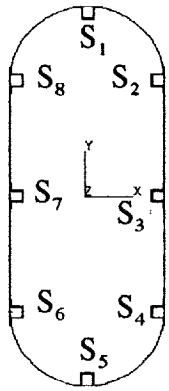

Fig. 4 Cross-sectional view of the structure showing the eight stringers

Furthermore, the moments of inertia of each stringer are assumed to be governed by the respective parallel axis components, and are easily expressed as a function of stringer cross-sectional area. Thus, stringers S_2, S_4, S_6 and S_8 are modeled using a single design variable for the cross sectional area. Likewise, one design variable is used for stringers S_1 and S_5 and another for stringers S_3 and S_7.

Each of the five circumferencial frames is assumed to have a uniform cross-sectional geometry, and treated by a single design variable for its cross-sectional area. The moments of inertia of each frame are also determined in a similar fashion as that described for the stringers.

Since the skin panels are defined based on the smeared properties of the composite laminates, it is sufficient to consider only the total thickness of a panel as a design variable. The four flat panels confined between two adjacent frames are modeled by a single design variable for thickness. Similarly, a single thickness design variable is used for the curved panels at the top and bottom. Consequently, eight design variables describe the thickness variation in the skin panels.

The total number of design variables for the panel thickness remains the same for both monolithic and sandwich cases, as both are modeled using PSHELL property cards and 2D anisotropic MAT 2 material cards in MSC/NASTRAN.

Figure 5 shows a pictorial view of the 16 variables that govern the design of the semi-monocoque structure. The stringer design variables are designated as S_1, S_2 and S_3 in units of in^2. The frame design variables are identified as F_1 through F_5 in units of in^2. The flat and curved skin panel thickness variables are identified as FP_1 through FP_4, and CP_1 through CP_4, respectively, measured in inches.

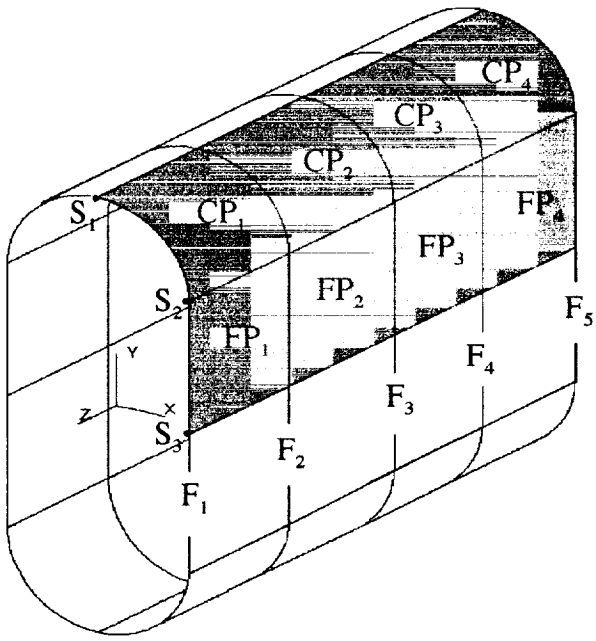

Fig. 5 Visual description of the design variables

The upper and lower bounds (i.e., side constraints) on the design variables are given in Table 3.

Table 3. Side constraints on design variables

Variable	Lower Bound	Upper Bound
Thickness[a], in.	0.100	0.500
Core Thickness, in.	0.054	0.594
Face sheet Thickness, in.	0.003	0.033
Stringer Area, in^2	0.240	1.430
Frame Area, in^2	0.188	0.940

[a]monolithic skin

Design Constraints

Two types of strength constraints are imposed on the design model: a maximum-stress constraint on each stringer and frame element, and a maximum-strain constraint on each two-dimensional skin element. There is also an additional buckling constraint imposed on the individual flat panels. For the curved panels, a conservative strain value is used as a buffer against buckling.

A margin of safety (MS) of 25% is used for the curved panels in compression and 10% for those in tension. Maximum strain values on flat panels are specified with MS = 10% in both tension and compression. Similarly, the frames and stringers have an MS of 25% in compression and 10% in tension.

The panel buckling constraints are set up in MSC/NASTRAN using the DEQATN cards. These cards contain the response equations as well as the equations to average the element forces and the stress interaction formula. Due to the variability of N_z and N_{yz} along the edges of each panel, the

corresponding average values are used for buckling assessment. In this case, a DRESP2 card is used to relate the thickness design variable and its element force, identified by the DRESP1 card, to the corresponding DEQATN card. There are sixteen DRESP2 cards for each of the sixteen flat panels.

The design space is defined by 3,256 design constraints and 32 side constraints. More specifically, there are 648 maximum-stress, 2,592 maximum-strain and 16 panel buckling constraints.

Optimization Results

The numerical results described in this section correspond to the external loads of magnitudes M_x = 4.095E5 in-lb, M_y = 2.18E5 in-lb and M_z = 1.22E5 in-lb.

Monolithic-Skin Structure

In this case, the design converged after ten iterations to an optimal weight of 183.5 lb. The distribution of the optimal design variables is shown in Fig. 6. Of all the 16 design variables, those defining the thickness of flat and curved panels are found to have a more significant effect on the structural weight.

The average thickness of the flat panels is three times larger than that of the curved panels. The constraints on the curved panels are satisfied with a thickness of approximately 20% to 40% larger than the minimum gage value. The higher thickness values for the flat panels are due to the buckling constraints. This observation was confirmed by seeing the flat panels come close to their minimum gage values when the buckling constraints were turned off in the optimization analysis. In fact almost all the design variables were close to their lower bounds in the absence of the buckling constraints although the loads were kept the same.

As a post-optimization check, both curved and flat panels were tested for buckling instability using MSC/NASTRAN. The results showed that none of the panels is susceptible to buckling at the optimum thickness.

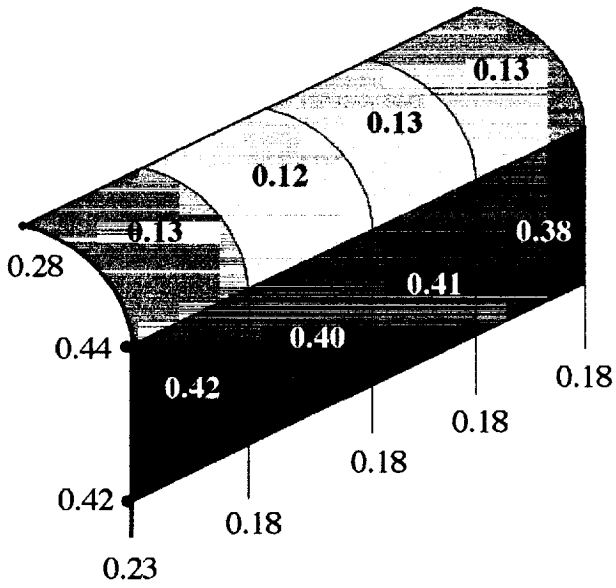

Fig. 6 Optimal design variables for the monolithic-skin structure

Except for the one near the loaded edge, all frames are at the minimum gage area. It appears that in this case only a minor portion of the internal loads is transferred to the frames.

Stringers S_2 and S_3 are found to be approximately 50% larger than S_1. This difference is due to the fact that S_2 and S_3 are more heavily loaded by the specified loading intensity.

Sandwich-Skin Structure

In this case, the design converged after six iterations to a minimum feasible weight of 119.8 lb. The distribution of the optimal design variables is shown in Fig. 7. The curved panels are pushed towards their maximum thickness of 0.66 in. As in the monolithic case, the panels located near the loaded edge are thicker than the other panels.

The cross-sectional areas of the frame are approximately two to three times the minimum gage values. It appears that a more significant portion of the load is being transferred to the frames in this case than in the monolithic case.

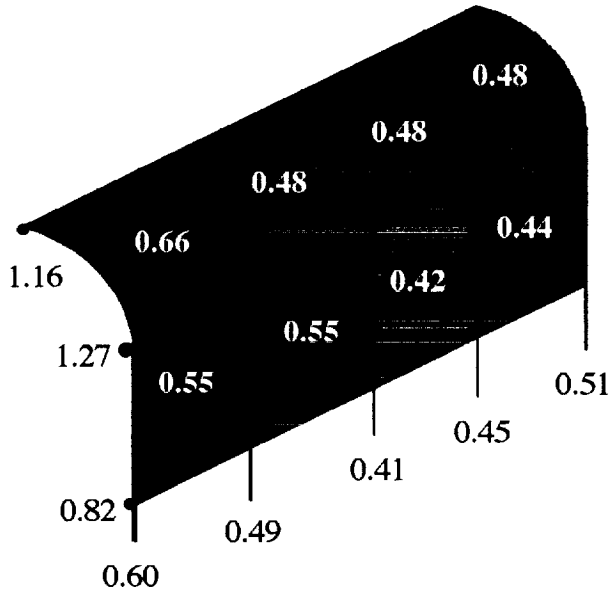

Fig. 7 Optimal design variables for the sandwich-skin structure

The stringers are also found to have significantly larger areas than in the monolithic case. Similar to the previous case, the middle stringer (S_2) has the largest area. However, S_1 stringer is larger than S_3, which is the opposite of that found in the previous case.

At the first glance, the increase in structural element sizing may appear counter-intuitive in the presence of thicker sandwich panels. However, a careful scrutiny of the structure identifies the reasons behind it.

Although, the sandwich panels are thicker than their counterparts in the monolithic case, they are not as heavy and stiff. We recall that 90% of the panel thickness comes from the aluminum honeycomb core. And if we were to compare the thickness of the top and bottom carbon-epoxy face sheets in each panel to the total thickness of the corresponding monolithic skin panel, we find that it is significantly thinner. Consequently, the thicker sandwich skin has a lower bending and extension stiffness than the monolithic skin, and the need for higher axial stiffness has led to the increase in

the cross-sectional areas of the stiffeners. For example, comparing the axial and bending stiffness values of the 0.42-in. monolithic panel with its 0.557-in sandwich counterpart, we obtain the following ratios:

$$A11_m/A11_s = 7.0 \qquad D11_m/D11_s = 1.6$$
$$A22_m/A22_s = 7.0 \qquad D22_m/D22_s = 1.4$$
$$A12_m/A12_s = 7.0 \qquad D12_m/D12_s = 1.7,$$

which clearly indicate the reason for large-size stiffeners in the sandwich design case. The A and D matrices are shown in the appendix.

Residual Strength Assessment

The residual strength of the structure is determined as the percentage of the design load it is capable of supporting when damaged. The strain energy density distribution is used as a means of identifying the regions of the structure that are most susceptible to failure. The strain energy density contour plot in Fig. 8 indicates the two regions, identified by *A* and *B*, as the most critical for the bending-torsion loading condition considered.[6] Region A is under combined tension and shear while region B is under combined compression and shear.

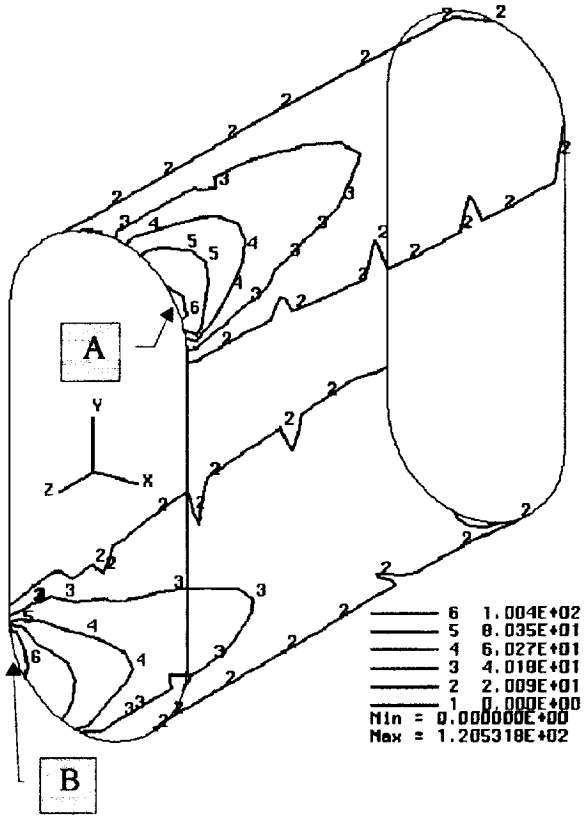

Fig. 8 Strain energy density contours for the cylindrical structure

In this study, we chose to introduce one type of damage in two possible forms in the vicinity of a critical region. In the first case, we considered damage in the form of skin-stringer joint failure causing detachment of stringer from the skin. In the second case, we modeled damage in the form

of skin-stringer-frame failure by detaching both stringer and frame from the skin. In both cases, buckling instability is used as the failure index for the whole structure.

Since buckling is used as the failure criterion, the panel where region B is located is used for damage placement and residual strength measurement. The stiffened panel, as shown in Fig. 9, consists of a flat and a curved skin section, two frames and three stringers.

Since the strain energy distribution pattern for the structural model with sandwich skin panels is identical to that with the monolithic skin, the same stiffened panel is used for the estimation of residual strength in both cases.

The stiffened panel, in Fig. 9, is analyzed for buckling using MSC/NASTRAN. The internal load and edge displacement information is obtained from the static finite element analysis of the optimal design for each skin concept. The global edge displacements are used in the buckling eigenvalue analysis of the stiffened panel.

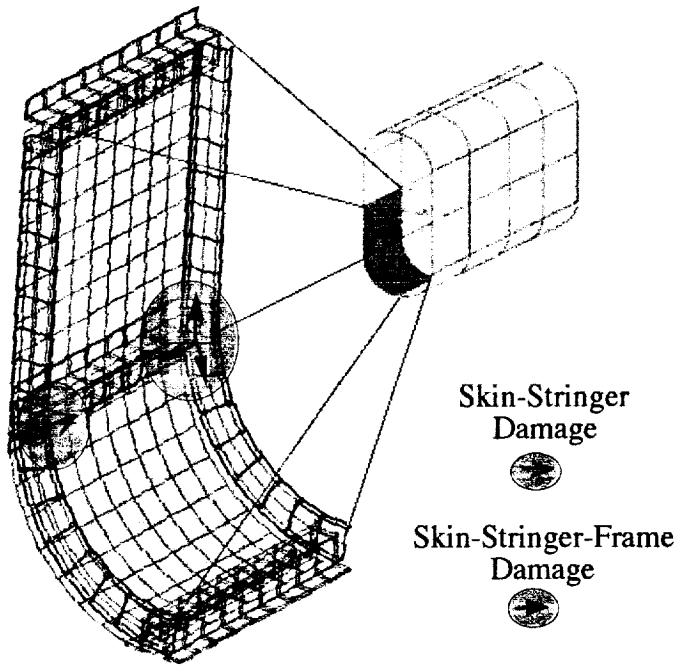

Fig. 9 Wire frame drawing of the stiffened panel showing the location and direction of damage growth

First, we considered the skin-stringer detachment in the area designated as the damage location in Fig. 9. The nodes common between the skin and stringer elements were duplicated to represent the joint separation. The size of damage was controlled by the number of nodes duplicated along the length of the stringer. A single node separation was used to model the smallest possible damage at a 2-in. distance from the left side corresponding to the loaded edge of the cylinder. The damage was then gradually increased in length along consecutive nodes toward the right edge of the panel.

To assess the effect of damage on the buckling characteristics of the panel, a linear static analysis was performed on the whole cylinder with damage. The displacement field was then applied along the edges of the panel for a local finite element buckling analysis.

For the monolithic case, no noticeable reduction in strength was observed up to a detachment length of 6 in., at which point the residual strength was found to be 87%. This indicates that the damaged structure is capable of supporting 87% of the design loads applied to the undamaged structure. For the sandwich case, no noticeable decrease was found up to a detachment length of 12 in., at which point the residual strength was found to be 92%.

The second form of damage as in skin-stringer-frame detachment was introduced next. The location of damage is shown in Fig. 9 with the direction of growth indicated by solid arrows.

For the monolithic case, a detachment length of 6 in. along the stringer and 4 in. along the frame results in a residual strength of 95%. For the sandwich case, a detachment length of 12 in. along the stringer and 4 in. along the frame results in a residual strength of 95%.

The skin-stringer-frame detachment is found to result in a higher residual strength value than the skin-stringer detachment. This is only because the skin-stringer detachment was modeled in the critical zone near the loaded edge whereas the skin-stringer-frame detachment was at some distance away from the critical zone near the right edge of the panel.

Conclusions

This report presented the results of an investigation to apply an efficient technique for addressing local skin buckling in design optimization of aircraft structures. The response surface methodology was used to determine the coefficients of algebraic polynomials that described the buckling behavior of rectangular skin panels with a high degree of accuracy. These polynomials were then used to formulate skin buckling constraints in MSC/NASTRAN through DEQATN cards .

The described technique was successfully applied to the design optimization of a semi-monocoque cylindrical structure under a combined bending-torsion loading condition. Both monolithic and sandwich skin design concepts were considered.

The main factor driving the design was found to be the buckling constraints associated with the flat panels. In addition, the design with a sandwich skin resulted in a structure that is approximately 35% lighter than that with a monolithic skin. This in spite of the fact that the stringers and frames supporting the structure with the sandwich skin are considerably larger than those in the monolithic skin design case.

A post-optimization residual strength calculation was used as a means of damage tolerance assessment of the optimal design configurations. For both skin-stringer and skin-stringer-frame damage configurations the sandwich skin design appeared to be more damage tolerant than its monolithic counterpart.

Future Work

The future research will consider the expansion of design requirements to include reliability as well as a more comprehensive treatment of damage initiation and propagation in the structure.

References

1. Ragon, S.A., Gurdal, Z., Haftka, and R.T., Tzong, T.J., "Global/Local Structural Wing Design Using Response Surface Techniques," Proceedings of the 38th AIAA/ASME/ASCE/AHS/ASC Structures, Structural Dynamics and Materials Conference and Exhibit, Kissimmee, FL, April 7-10, 1997, pp 1204-1215.
2. Giunta, A.A. and Watson, L.T., "A Comparison of Approximation Modeling Techniques: Polynomial Versus Interpolating Models," Proceedings of the 7th AIAA/USAF/NASA/ISSMO

Symposium on Multidisciplinary Analysis and Optimization, St. Louis, MO, September 2-4, 1998, pp. 392-4004.
3. Papila, M. and Haftka, R.T., "Uncertainty and Wing Structural Weight Approximations," 40th AIAA/ ASME/ASCE/AHS/ASC Structures, Structural Dynamics and Materials Conference and Exhibit, St. Louis, MO, April 12-15, 1999, pp. 988-1002.
4. Cruz, J.R., SCBUCKLE Users Manual, NASA Technical Memorandum 107741, March 1993.
5. Whitney, J.M., Structural Analysis of Laminated Anisotropic Plates, Technomic Publishing Co., Inc., 1987, pp. 87-131
6. Sih, G.C., and MacDonald. B., "Fracture Mechanics Applied to Engineering Problems – Strain Energy Density Criterion," *Engineering Fracture Mechanics*, Vol.6, 1974, pp. 361-386.

Appendix

The stiffness matrices for the monolithic skin at t = 0.42 in.:

THE AXIAL STIFFNESS MATRIX $[A]_m$

0.58404E+07	0.11087E+07	0.00000E+00
0.11087E+07	0.38044E+07	0.00000E+00
0.00000E+00	0.00000E+00	0.13919E+07

THE BENDING STIFFNESS MATRIX $[D]_m$

0.86497E+05	0.18349E+05	0.31425E+04
0.18349E+05	0.51181E+05	0.31425E+04
0.31425E+04	0.31425E+04	0.22511E+05

The stiffness matrices for the sandwich skin at t = 0.557 in. with the core properties ignored in the stiffness calculations:

THE AXIAL STIFFNESS MATRIX $[A]_s$

0.77316E+06	0.14677E+06	0.00000E+00
0.14677E+06	0.50363E+06	0.00000E+00
0.00000E+00	0.00000E+00	0.18426E+06

THE BENDING STIFFNESS MATRIX $[D]_s$

0.54162E+05	0.10286E+05	0.00000E+00
0.10286E+05	0.35269E+05	0.00000E+00
0.00000E+00	0.00000E+00	0.12912E+05

The stiffness matrices for the sandwich skin at t = 0.557 in. with the core properties <u>included</u> in the stiffness calculations:

THE AXIAL STIFFNESS MATRIX $[A]_s$

0.84665E+06	0.15780E+06	0.00000E+00
0.15780E+06	0.54038E+06	0.00000E+00
0.00000E+00	0.00000E+00	0.21183E+06

THE BENDING STIFFNESS MATRIX $[D]_s$

0.55701E+05	0.10517E+05	0.00000E+00
0.10517E+05	0.36039E+05	0.00000E+00
0.00000E+00	0.00000E+00	0.13490E+05

$A11_m/A11_s = 6.9$
$A22_m/A22_s = 7.0$
$A12_m/A12_s = 7.0$

$D11_m/D11_s = 1.6$
$D22_m/D22_s = 1.4$
$D12_m/D12_s = 1.7$